Supporting Information for

A Family of Heterometallic Semicircular $Mn^{III}_2Ln^{III}_3$ Strands

Muhammad Nadeem Akhtar, Yan-Zhen Zheng, Yanhua Lan, Valeriu Mereacre, Christopher E. Anson and Annie K. Powell*

Institut f¨ur Anorganische Chemie, Universit¨at Karlsruhe (TH), Engesserstrasse Geb. 30.45 76128 Karlsruhe, Germany.

Fax: +49-721-6088142

e-mail: powell@aoc.uni-karlsruhe.de (A.K.P.)

Experimental Section

General considerations

All the reactions were carried out under aerobic condition and all $Ln(NO_3)_3.XH_2O$ were prepared by dissolving lanthanides oxides in concentrated nitric acid respectively. The N-butyldiethanolamine (N-bdea) and $Mn(OAc)_2{\cdot}4H_2O$ and other reagents were obtained from commercial sources and used without further purification. IR spectra were measured on Perkin Elmer Spectrum One spectrometer with samples prepared as KBr discs. Elemental analyses for C, H and N were carried out at the Institute for Inorganic Chemistry at the University of Karlsruhe.

Synthesis

Synthesis of **1**: A solution of $bdeaH_2$ (0.64 g, 4.0 mmol) in 10 ml of MeCN and $Y(NO_3)_3.6H_2O$ (0.22 g, 0.5 mmol) were added to a stirred solution of $Mn(OAc)_2.4H_2O$ (0.12 g, 0.5 mmol) and pivalic acid (0.20 g, 2.0 mmol) in 10 ml of MeCN, resulting in a dark brown solution. After 48 h, brown crystals were collected by filtration, washed with acetonitrile. Yield 25% (based on Mn). Anal. Calcd for $C_{82}H_{163}Mn_2Y_3N_6O_{26}$ (**1**): $C_{82}H_{163}Mn_2Y_3N_6O_{26}$ (**1**): C, 48.62; H, 8.11; N, 4.15. Found: C, 48.45; H, 7.95, N, 4.08. IR (KBr, cm^{-1}) 3425(b), 3073(m), 2959 (vs), 2928(s), 1580(s), 1550(vs), 1482(vs), 1411(vs), 1374(s), 1227(s), 1088(s), 907(m), 792(w), 746(w), 638(s), 606(m), 550(w). **2** was prepared similarly to **1** but using $Tb(NO_3)_2.6H_2O$. Yield 20% (based on Mn). Anal. Calcd for $C_{82}H_{163}Mn_2Tb_3N_6O_{26}$ (**2**): C, 44.05; H 7.35; N, 3.76. Found: C, 44.24; H, 7.23; N 3.45. IR (KBr, cm^{-1}): 3431 (b), 2958(vs), 2930(s), 1583(s), 1549(vs), 1483(vs), 1411(vs), 1372(s), 1358(s), 1225(s), 1089(s), 908(m), 895(m), 807(w), 744(w), 636(s), 606(m), 551(w). **3** was prepared similarly to **1** but using $Dy(NO_3)_2.6H_2O$. Yield 19% (based on Mn). Anal. calcd for $C_{82}H_{163}Dy_3Mn_2N_6O_{26}$ (**3**): C, 43.84; H 7.31; N, 3.74. Found: C, 43.50; H, 7.09; N 3.57. IR (KBr, cm^{-1}) 3426(b), 2960 (vs), 2867(s), 1583(s), 1549(vs), 1483(vs), 1461(m), 1412(vs), 1372(s), 1225(s), 1089(s), 1012(w), 908(m), 807(w), 744 (w), 638(s), 607(m), 552(w). **4** was prepared similarly to **1** but using $Ho(NO_3)_2.6H_2O$. Yield 18% (based on Mn). Anal. calcd for $C_{82}H_{163}Ho_3Mn_2N_6O_{26}$: C, 43.70; H 7.29; N, 3.73. Found: C, 43.51; H, 7.12; N, 3.72. IR (KBr, cm^{-1}) 3443(b), 2961(vs), 2866(s), 1582(s), 1548(vs), 1482(vs), 1414(vs), 1372(s), 1225(s),

1092(s), 909(m), 791(w), 745(w), 650(s), 608(m), 494(w). **5** was prepared similarly as **1** but using $Er(NO_3)_2.6H_2O$. Yield 36% (based on Mn) Anal. Calcd for $C_{82}H_{163}Er_3Mn_2N_6O_{26}$ (**5**): C, 43.56; H 7.27; N, 3.72. Found: C, 43.28; H, 7.11; N, 3.49. IR (KBr, cm^{-1}) 3462(b), 2960(vs), 2866(s), 1582(s), 1549(vs), 1482 (vs), 1414(vs), 1372(s), 1225(s), 1091(s), 909(m), 791(w), 743(w), 645(s), 607(m), 553(w), 492(w).

Crystal structure determinations

X-ray data were collected at 100k on a Bruker SMART Apex CCD diffractometer (**1 - 5**) using graphite-monochromated Mo-Kα radiation. Since the compounds are isostructural, only full determinations were carried out for **1**, **3** and **5**. Semi-empirical absorption corrections were made using SADABS[16a] The structures were solved using direct methods, followed by full matrix least-squares refinement against F^2 (all data) using SHELXTL[16b]. Anisotropic refinement for all ordered non-H atoms; orgainc H atoms were placed in calculated positions, while coordinates of hydroxo H atoms were refined.

Magnetic measurements

The magnetic susceptibility measurements on compounds **1-5** were obtained with the use of a Quantum Design SQUID magnetometer MPMS-XL. This magnetometer works between 1.8 and 400 k for dc applied fields ranging from -7 to 7. Measurements were performed on a polycrystalline sample of 9.9, 8.6, 14.2, 19.0 and 12.8 mg for complex **1, 2, 3, 4** and **5** respectively. ac susceptibility measurements were measured with an oscillating ac field of 3 Oe and ac frequencies ranging from 1 to 1500 Hz. M vs H measurements has been performed at 100 K to check for the presence of ferromagnetic impurities that has been found absent. The magnetic data were corrected for the sample holder and the diamagnetic contribution.

Based on the structure, the compound **1** can be viewed as a dimmer of Mn(III) due to the presence of the diamagnetic Y(III) ion. Therefore, to model the temperature behaviour of the magnetic susceptibility of this compound, I have used a simple isotropic Heisenberg dimer model of $S = 2$ spins with the following spin Hamiltonian:

$$H = 2JS_{MnA}S_{MnB} \quad (1)$$

where J is the exchange interactions in the dimer between Mn(III) ions as seen on the scheme above. The application of the van Vleck equation [J. H. van Vleck, *The Theory of Electric and Magnetic Susceptibility*, Oxford University Press, (1932).] to the Kambe's vector coupling scheme [K. Kambe, J. Phys. Soc. Jpn. 5 (1950) 48.], allows a determination of the low field analytical expression of the magnetic susceptibility:

$$\chi_{Mn_2} = \frac{Ng^2\mu_B^2}{k\,T} \cdot \frac{2e^{\frac{2J}{kT}} + 10e^{\frac{6J}{kT}} + 28e^{\frac{12J}{kT}} + 60e^{\frac{20J}{kT}}}{1 + 3e^{\frac{2J}{kT}} + 5e^{\frac{6J}{kT}} + 7e^{\frac{12J}{kT}} + 9e^{\frac{20J}{kT}}}$$

This model was able to reproduce well the experimental data in the full temperature range. The best set of parameters found is: J/k_B = -0.31(1) K, g = 2.08(1) and χ_{dia}= 3.1 10^{-4} cm^3mol^{-1}.

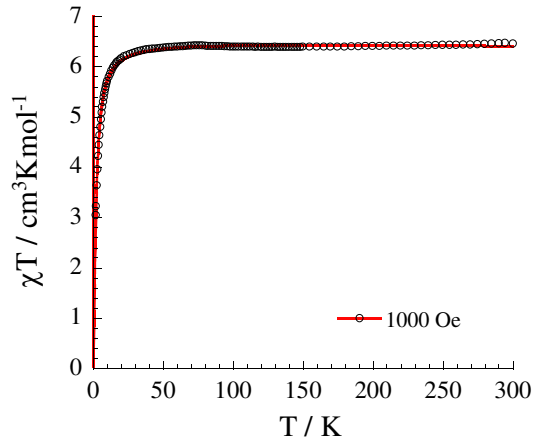

Figure **S1**: The χT vs T plot of compound **1**. open circles: experimental data; solid line (the fitting, see the above text).

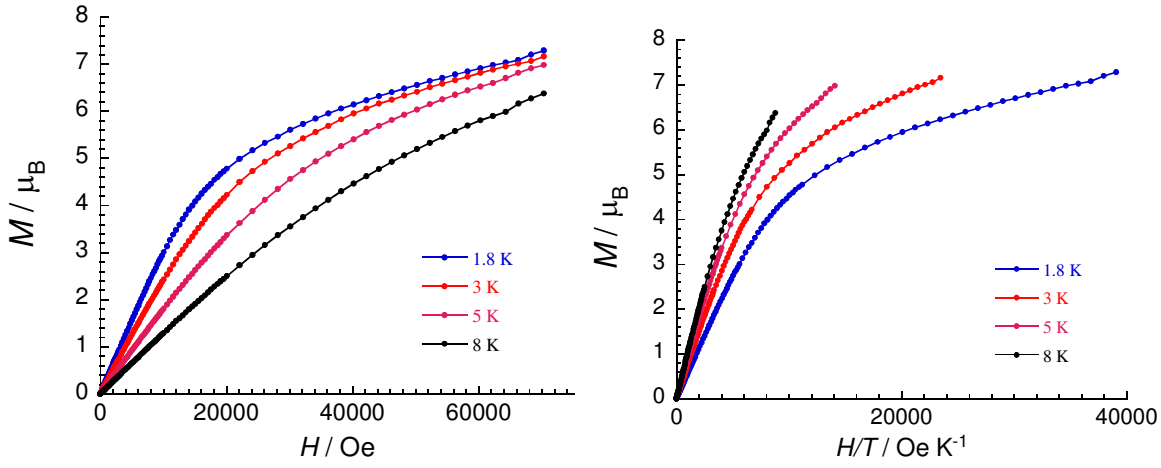

Figure S2. Field dependence of the magnetization of complex for **1**.

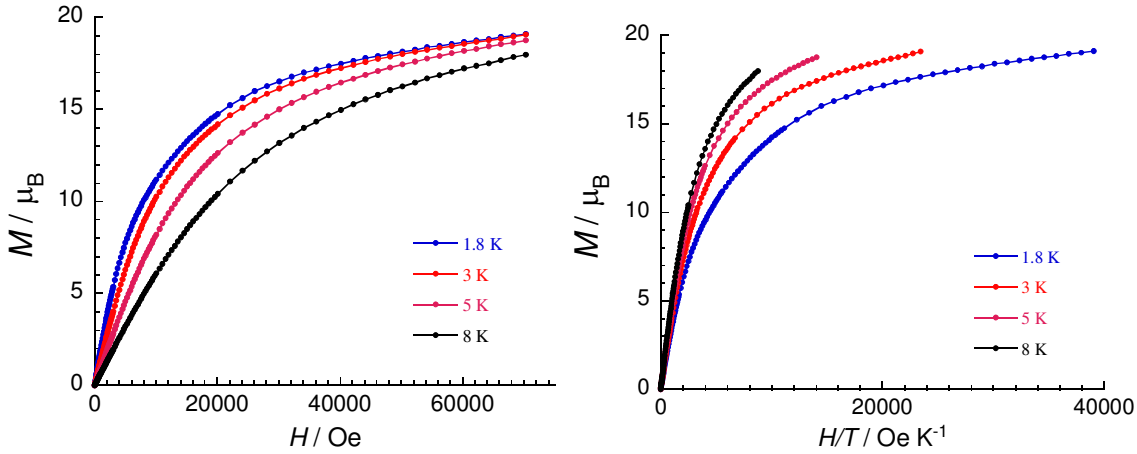

Figure S3. Field dependence of the magnetization of complex for **2**.

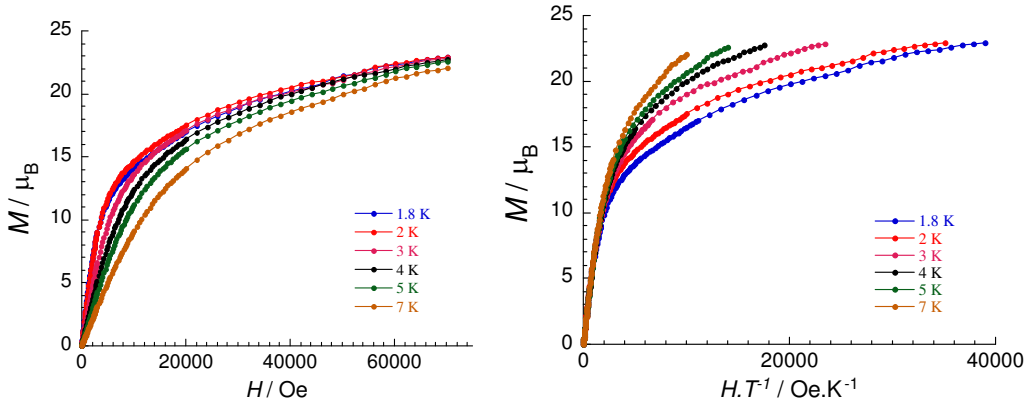

Figure S4. Field dependence of the magnetization of complex for **3**.

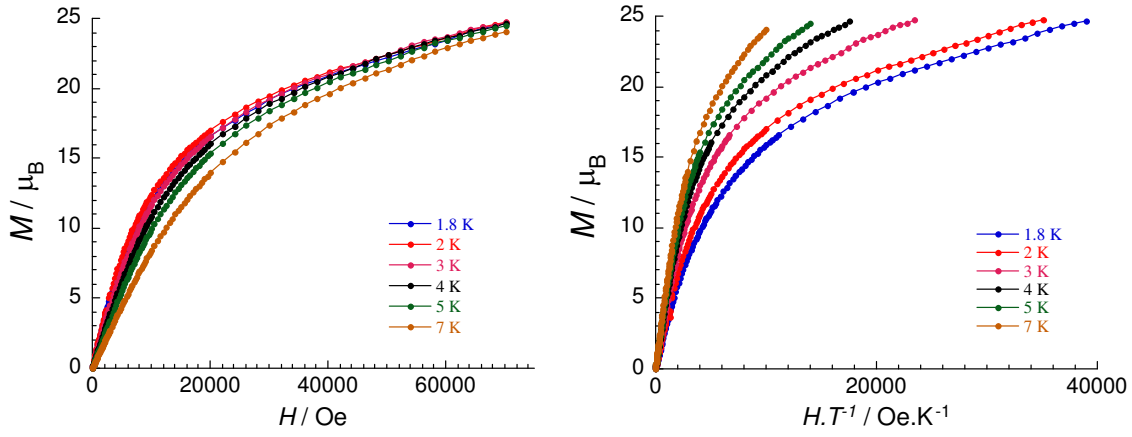

Figure S5. Field dependence of the magnetization of complex for **4**.

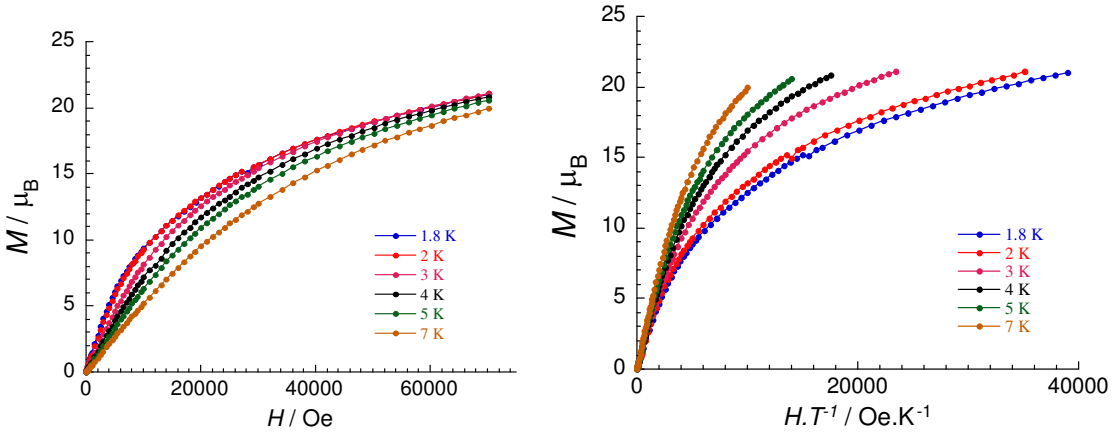

Figure S6. Field dependence of the magnetization of complex for **5**.